

# Dynamics of a two-degree-of-freedom cantilever beam with impacts

Barbara Blazejczyk-Okolewska <sup>\*</sup>, Krzysztof Czołczyński, Tomasz Kapitaniak

*Division of Dynamics, Technical University of Lodz, Stefanowskiego 1/15, 90-924 Lodz, Poland*

Accepted 19 September 2007

Communicated by Prof. L. Marek-Crnjac

---

## Abstract

Impacts in mechanical systems are an object of interest for many scientists in the world. In this paper, we present detailed investigations of the dynamical behavior of the system consisting of a massless cantilever beam with two concentrated masses. The maximum displacement of one of the masses is limited to the threshold value by a rigid stop, which gives rise to non-linearity in the system. Impacts between the mass and the basis are described by a coefficient of restitution. The conducted calculations show a good agreement of the results obtained with two qualitatively different methods of behavior analysis of the system under consideration, namely: the Peterka's method and the method of numerical integration of motion equations. It has been observed that stable solutions describing the motion with impacts of a two-degree-of-freedom mechanical system exist in significantly large regions of the parameters that describe this system. The location and size of periodic motion regions depend strongly on mutual relations between the excitation force frequency and the system eigenvalues. In order to obtain stable and periodic motion with impacts, the system parameters should be selected in such a way as to make the excitation force frequency an even multiple of the fundamental eigenvalue and to make the higher eigenvalue an even multiple of the excitation force frequency. These two conditions can be applied in designing mechanical systems with impacts. This information is even of more significance since it has turned out that the system exhibits some adaptability, owing to which stable solutions exist even if the above-mentioned conditions are satisfied only approximately.

© 2007 Elsevier Ltd. All rights reserved.

---

## 1. Introduction

Systems in which impacts of matching elements occur play an important role in the theory of vibration of mechanical systems. They became an object of investigation already in the mid 1950s and since then the interest in them has been still growing. It is not surprising as vibro-impact motion characterizes a large class of physical systems. For example, printing hammers, tooling machines, gear boxes, and heat exchangers all involve motion of an object which is limited by a stop.

---

<sup>\*</sup> Corresponding author. Tel.: +48 42 6312233; fax: +48 42 6365646.  
E-mail address: [okolbar@p.lodz.pl](mailto:okolbar@p.lodz.pl) (B. Blazejczyk-Okolewska).

A vibro-impact system is usually modeled as a spring-mass system with amplitude constraint. In a number of studies, one degree of freedom (1-DOF) has been used. Impact gives rise to nonlinearity and discontinuity so that vibro-impact systems can exhibit rich and complicated dynamic behavior. In recent years, dynamics of mechanical systems with impacts have been the subject of several investigations, and many new theoretical issues have been advanced in research of vibro-impact problems. From the viewpoint of application of impact oscillators, the regularity of their motion is of special importance. Therefore, regions of stable regular behaviors of such systems have become an object of extensive studies. Shaw and Holmes [36] analytically determined the stability of periodic solutions and identified chaotic features such as period-doubling, horseshoes and strange attractors. Moon and Shaw [28] considered a single-DOF approach to modeling a vibro-impact cantilever beam experiment, also by reducing the model to a single mode. In this case, the system was considered as piecewise linear, and the single-DOF model was obtained using the Galerkin method applied to each linear part. Further analysis and experimental studies were conducted by Shaw [35], who used a cantilever beam contacting a stiff stop to compare cases of moderate and large stiffness ratios (the ratio between the stiffness of the first beam bending mode and the stiffness at the stop). For the system, high damping to discourage contribution to the response from higher beam modes was considered. Experiment in this area was also conducted by Fang and Wickert [17], who used a cantilevered beam with a tip mass to demonstrate period-one, period-two and chaotic motion. A fundamental work devoted to the dynamical behavior of 1-DOF oscillator impacts is the study by Nordmark [29]. A survey of modern methods used for modeling systems with impacts and the analysis of their motion, a grazing incidence as a reason of non-periodic motion in an impact oscillator, effects of a low velocity impact, and also a comparison between numerical and experimental results was presented. Some classical, analytical investigations concerning impact oscillators and piecewise smooth systems were also carried out by Arnold [2], Ivanov [22] and Feigin [18]. The use of computers has enabled detailed studies of various phenomena, like chaotic motion, Feigenbaum scenario, sudden changes in a chaotic attractor intermittent to chaos, Devil's attractors and different types of grazing bifurcations or border-collision bifurcations. These phenomena were investigated, for example, by Blazejczyk-Okolewska et al. [5], Chin et al. [9], de Weger et al. [15], di Bernardo et al. [16], Isomaki et al. [23], Peterka and Vacik [33], Thomson and Ghaffari [37].

All of the mentioned works assume a 1-DOF system, and the corresponding experiments have been restricted to confirm this assumption as closely as possible. Studies on multi-DOF systems are more limited. Aidanpaa and Gupta [1] analyzed the one-sided impact motion of a 2-DOF impact vibrator. They studied an influence of system parameters and compared the dynamical response behavior of 2-DOF with that of a single-DOF. Van de Vorst et al. [38] built a finite element model and conducted an experiment involving a flexible beam supported by leaf springs at either end and contacting a Hertzian spring at its mid-point. Numerical and experimental results are shown to agree fairly well. Some special attention should be also drawn to the studies by Bapat [3], Cempel [8], Dabrowski [13], Masri [26], Masri and Caughey [27], Popplewell and Liao [34], Peterka [31], Peterka and Blazejczyk-Okolewska [32] that include numerical, theoretical and experimental analyses of vibro-impact dampers, by Koizumi [25] and Park [30] that describe the application of impact oscillators as models of molding machines, by Blazejczyk-Okolewska et al. [5], Foale and Bishop [19] as well as Hinrichs et al. [21] that comprise the investigations on the effect of dry friction on responses of simple models of mechanical systems with impacts. In solving the problem of seeking regions of the existence of periodic motion with impacts of 2-DOF systems, the method presented by Peterka [31], below referred to as the "Peterka's method", turned out to be very useful. This method applied to systems composed of two oscillators in series was presented in [1]. The application of this method for a system that consists of two independent oscillators and some exemplary results of the numerical studies that confirm its correctness and usefulness have been shown by Czolczynski and Kapitaniak in [10–12].

The number of these studies is a proof of universality of the impact phenomenon that occurs in various technical devices (e.g., see [24] and the references therein) and of importance of computer modeling of such devices. While describing the phenomena that take place in vibro-impact systems (e.g., see [7,20]), one can encounter some difficulties in modeling an impact. This phenomenon can be modeled in various ways depending on the physical conditions that are to be considered (generally, two approaches are known, namely: (i) impact oscillators which assume an instantaneous contact with a coefficient of restitution model, (ii) piecewise systems, which model the contact as a linear or Hertzian spring, leading to separate equations of motion for in and out of contact cases). To model the system in the interval between impacts, two extreme approaches are commonly used, that is to say: a model consists of light elastic elements and rigid elements with inertia, or a model has a form of an elastic element only, with a continuous and uniform mass distribution, and an impact occurs directly against this element. In the latter model, there are no rigid mass elements. Let us notice that during motion of systems with impacts, their trajectories can tend to one of a few co-existing attractors (e.g., see [6]). Neglecting masses of elastic elements can lead to a wrong determination of asymptotic solutions to motion equations and, due to sensitivity to initial conditions (e.g., see [6,14]), to a false identification of the attractor the trajectory tends to. Another important aspect is a prediction of the nature of motion of a system with impacts: whether it is going to be regular (periodic), or rather chaotic – so fashionable nowadays but not necessarily bringing happiness to the designer of industrial devices. Simple calculations show that inconsiderate negligence of the spring mass (and a

limitation in the number of degrees of freedom that follows) can lead to a false identification of those regions of parameters for which the system motion is periodic.

And thus a problem arises: which physical model is suitable for computer-aided-design of systems in which there are both a heavy rigid element and a spring of a considerable mass (which requires additional degrees of freedom to be taken into consideration in the model)? In initial analysis of this system, a physical model of the beam or the elastic weightless shaft that carries a finite number of concentrated bodies can be used. The present study includes analytical investigations of the 2-DOF system, connected adequately by means of elastic structures (the way of connection complies with the principles of classification of mechanical systems with impacts described by Blazejczyk-Okolewska et al. in [4]). The maximum displacement of one of the masses is limited to the threshold value by a rigid stop, which gives rise to non-linearity in the system. Impacts between the mass and the basis are described by a coefficient of restitution. In the calculations, two qualitatively different methods of the analysis of behavior were used, namely: the Peterka’s method [31] and the method of numerical integration of motion equations. During the investigations, special attention was paid to the determination of regions of periodic motion with impacts and stability of periodic solutions. This analysis will be helpful in modeling systems with impacts of non-negligibly high mass of elastic elements. In further investigations, the number of concentrated masses in the system will be increased to such a number that will enable us to obtain a good agreement with the results obtained with the finite element method when introduced into the calculations of motion equations by means of the numerical integration method. In the future, the authors are going to compare the results obtained with experimental results as well.

## 2. Physical and mathematical model of the system

The object under investigation is a 2-DOF vibrating system presented in Fig. 1a. The system is composed of two concentrated masses  $m_1$  and  $m_2$  connected with a basis by means of light linear springs with coefficients of stiffness  $k_1$  and  $k_2$ . Additionally, the masses are connected with each other by means of a spring with a coefficient of stiffness  $k_{12}$ . Because of the existence of the spring  $k_1$ , the system under consideration differs from classical 2-DOF vibrating systems, whose dynamical behavior was considered in previous publications (e.g., see [1]). The spring  $k_1$  has been introduced so that in the mathematical model of the system under analysis there are three coefficients of stiffness, that is to say, their number is equal to the number of different terms in the symmetrical stiffness matrix of the 2-DOF mechanical system. Let us notice that the spring system, which will thus arise, will be the *basic spring 2-DOF system*, according to the principles of classification of mechanical systems with impacts described in [4]. It is worth mentioning that thanks to it, the system under analysis can be used, for instance, to investigate the dynamical behavior of the system consisting of a massless cantilever beam with two concentrated masses. In the simplified (discrete) physical model, the mass  $m_2$  can represent the existing (positive) beam mass in the real system. The mass  $m_1$  has a fender that can impact against the basis during motion. If the system is in the static equilibrium position, then the lower part of the mass  $m_1$  (fender) is at the distance  $\bar{d}$  from the basis. A harmonic excitation force, whose amplitude is proportional to the square of

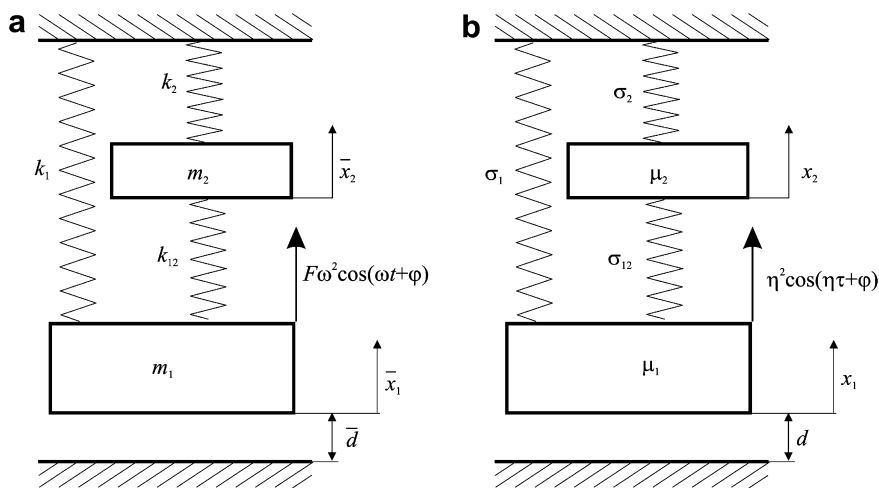


Fig. 1. 2-DOF system with impacts and external excitation; (a) dimensional form; and (b) dimensionless form.

its circular velocity, acts on the mass  $m_1$  – like in the case of a force excited by the centrifugal force acting on the rotating rotor.

In the time intervals between impacts, the motion of the system presented in Fig. 1a is described by the following equations

$$\begin{aligned} m_1 \frac{d^2 \bar{x}_1}{dt^2} + (k_1 + k_{12}) \bar{x}_1 - k_{12} \bar{x}_2 &= F \omega^2 \cos(\omega t + \varphi), \\ m_2 \frac{d^2 \bar{x}_2}{dt^2} - k_{12} \bar{x}_1 + (k_2 + k_{12}) \bar{x}_2 &= 0. \end{aligned} \quad (1)$$

While trying to write these equations in the dimensionless form, a problem of selection of the vibrating 1-DOF system, whose mass and coefficient of stiffness (and hence, the frequency of natural vibrations) would be the reference quantities for masses and coefficients of stiffness of the 2-DOF system, arose. It was decided it would be the system presented in Fig. 2, with the following values of mass and stiffness

$$\begin{aligned} k &= k_1 + \frac{k_{12} k_2}{k_{12} + k_2}, \\ m &= m_1 + m_2, \\ \alpha^2 &= \frac{k}{m}. \end{aligned} \quad (2)$$

Multiplying Eq. (1) by  $m$  and dividing it by  $kF$ , after some simple transformations we obtain dimensionless equations of motion

$$\begin{aligned} \mu_1 \ddot{x}_1 + \sigma_1 x_1 - \sigma_{12} x_2 &= \eta \cos(\eta \tau + \varphi), \\ \mu_2 \ddot{x}_2 - \sigma_{12} x_1 + \sigma_2 x_2 &= 0, \end{aligned} \quad (3)$$

where

$$\begin{aligned} \mu_1 &= m_1/m, \quad \mu_2 = m_2/m, \quad \sigma_1 = (k_1 + k_{12})/k, \quad \sigma_2 = (k_2 + k_{12})/k, \quad \sigma_{12} = k_{12}/k, \quad \eta = \omega/\alpha, \\ \tau &= \alpha t - \text{dimensionless time,} \\ x_1 &= \bar{x}_1 m/F, \quad x_2 = \bar{x}_2 m/F - \text{dimensionless displacements,} \end{aligned}$$

$$\ddot{x}_1 = \frac{d^2 x_1}{d\tau^2}, \quad \ddot{x}_2 = \frac{d^2 x_2}{d\tau^2},$$

$d = \bar{d} m/F$  – dimensionless distance between the impacting surface of the mass  $m_1$  and the basis.

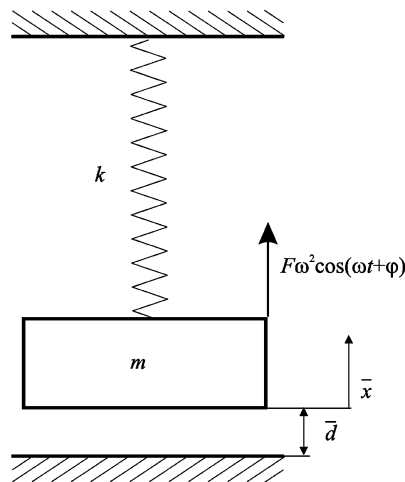


Fig. 2. System of reference.

Fig. 1b shows the system under analysis in the dimensionless form. The impact of the mass  $m_1$  with the basis is modeled applying the well-known Newton's law

$$v_1^+ = -k_r v_1^-, \tag{4}$$

where  $v_1^-$  denotes the velocity before impact and  $v_1^+$  – the velocity after impact;  $k_r$  is the coefficient of restitution.

To integrate Eq. (3), the Runge–Kutta method was employed; the moments of impacts were established using the method of successive approximations. Eqs. (3) and (4) provide information on the system behavior in the form of time series, phase planes, Poincare maps and bifurcation diagrams.

### 3. Periodic solutions

From the designer's point of view, the information for which sets of parameters characterizing the system  $(\mu_1, \mu_2, \sigma_1, \sigma_2, \sigma_{12}, \eta, k_r, d)$  its motion is periodic is essential. In order to acquire this information, we can apply the so-called Peterka's method [31]. In its original form, this method could be used for 1-DOF oscillators with impacts, or to the systems consisting of two identical oscillators impacting each other. The authors have generalized this method in numerous ways, which have been discussed in previous publications (see [10–12] and the references therein). Below, a successive variant of this method, determined for the system of oscillators under consideration, is presented.

As it is known, the solutions to Eq. (3) can be written in the form

$$\begin{aligned} x_1(\tau) &= A_{11} \cos(\alpha_1 \tau + \psi_1) + A_{12} \cos(\alpha_2 \tau + \psi_2) + B_1 \cos(\eta \tau + \varphi), \\ x_2(\tau) &= A_{21} \cos(\alpha_1 \tau + \psi_1) + A_{22} \cos(\alpha_2 \tau + \psi_2) + B_2 \cos(\eta \tau + \varphi). \end{aligned} \tag{5}$$

The eigenvalues  $\alpha_1, \alpha_2$  of the system can be obtained as the roots of the characteristic equation

$$(\sigma_1 - \mu_1 \alpha^2)(\sigma_2 - \mu_2 \alpha^2) - \sigma_{12}^2 = 0. \tag{6}$$

They can be expressed as follows

$$\alpha_{1,2}^2 = \frac{(\sigma_1 \mu_2 + \sigma_2 \mu_1) \mp \sqrt{A}}{2\mu_1 \mu_2},$$

where

$$A = (\sigma_1 \mu_2 + \sigma_2 \mu_1)^2 - 4\mu_1 \mu_2 (\sigma_1 \sigma_2 - \sigma_{12}^2).$$

The relations between the amplitudes of free vibrations are given by the eigenvectors

$$\begin{aligned} \Phi_1 &= \frac{A_{21}}{A_{11}} = \frac{\sigma_1 - \mu_1 \alpha_1^2}{\sigma_{12}}, \\ \Phi_2 &= \frac{A_{22}}{A_{12}} = \frac{\sigma_1 - \mu_1 \alpha_2^2}{\sigma_{12}}. \end{aligned} \tag{7}$$

The amplitudes of forced vibrations are written as

$$\begin{aligned} B_1 &= \frac{\eta^2 (\sigma_2 - \mu_2 \eta^2)}{(\sigma_1 - \mu_1 \eta^2)(\sigma_2 - \mu_2 \eta^2) - \sigma_{12}^2}, \\ B_2 &= \frac{\eta^2 \sigma_{12}^2}{(\sigma_1 - \mu_1 \eta^2)(\sigma_2 - \mu_2 \eta^2) - \sigma_{12}^2}. \end{aligned} \tag{8}$$

While seeking the conditions which must be fulfilled to yield periodic motion of the system with impacts, it was assumed that the time interval between two subsequent impacts is equal to a multiple of the forcing period  $T = \frac{2\pi}{\eta}$ , which means

$$\begin{aligned} x_1(0) &= x_1\left(\frac{2\pi n}{\eta}\right), \\ x_2(0) &= x_2\left(\frac{2\pi n}{\eta}\right), \end{aligned} \tag{9}$$

where  $n = 1, 2, 3, \dots$

Introducing (3) into (9) and employing (7), it can be found that

$$\begin{aligned}\psi_1 &= -\frac{\pi n \alpha_1}{\eta}, \\ \psi_2 &= -\frac{\pi n \alpha_2}{\eta}.\end{aligned}\quad (10)$$

The equations describing the relations between velocities

$$\begin{aligned}v_1(0) &= -k_r v_1 \left( \frac{2\pi n}{\eta} \right), \\ v_2(0) &= v_2 \left( \frac{2\pi n}{\eta} \right)\end{aligned}\quad (11)$$

provide (together with Eq. (7)) the system of two equations

$$\begin{bmatrix} a_{11} & a_{12} \\ a_{21} & a_{22} \end{bmatrix} \begin{Bmatrix} A_{11} \\ A_{12} \end{Bmatrix} = \begin{Bmatrix} b_1 \\ b_2 \end{Bmatrix}\quad (12)$$

where

$$\begin{aligned}a_{11} &= -\alpha_1 \left[ \sin \psi_1 + k_r \sin \left( \frac{2\pi n}{\eta} \alpha_1 + \psi_1 \right) \right], \\ a_{12} &= -\alpha_2 \left[ \sin \psi_2 + k_r \sin \left( \frac{2\pi n}{\eta} \alpha_2 + \psi_2 \right) \right], \\ a_{21} &= \alpha_1 \Phi_1 \left[ \sin \left( \frac{2\pi n}{\eta} \alpha_1 + \psi_1 \right) - \sin \psi_1 \right], \\ a_{22} &= \alpha_2 \Phi_2 \left[ \sin \left( \frac{2\pi n}{\eta} \alpha_2 + \psi_2 \right) - \sin \psi_2 \right], \\ b_1 &= (1 + k_r) \eta \sin \varphi, \\ b_2 &= 0,\end{aligned}$$

and from which we can obtain two formulas describing the unknown amplitudes of free oscillations  $A_{11}$  and  $A_{12}$  as functions of the phase shifting  $\varphi$ . After substituting these formulas and solution (3) into the condition of impact

$$x_1(0) = -d,\quad (13)$$

we can determine the phase shifting  $\varphi$  as the unknown in the equation

$$K_s \sin \varphi + K_c \cos \varphi + d = 0,\quad (14)$$

where

$$\begin{aligned}K_c &= B_1, \\ K_s &= \frac{a_{22} \cos \psi_1 - a_{21} \cos \psi_2}{a_{11} a_{22} - a_{12} a_{21}} (1 + k_r) \eta B_1.\end{aligned}$$

Having performed some simple transformations, we obtain the solution to Eq. (14) in the form

$$\begin{aligned}\sin \varphi &= \frac{-dK_s + K_c \sqrt{K_s^2 + K_c^2 - d^2}}{K_s^2 + K_c^2}, \\ \cos \varphi &= \frac{-dK_c - K_s \sqrt{K_s^2 + K_c^2 - d^2}}{K_s^2 + K_c^2}.\end{aligned}\quad (15)$$

Substituting (15) into the formulas describing  $A_{11}$  and  $A_{12}$  as functions of the phase shifting  $\varphi$ , we can finally calculate these amplitudes. There exists, of course, another pair of solutions (15) as well, with the opposite signs in front of the root, however its substitution yields (as it appeared during the numerical calculations) an unstable solution to the equation of motion. Therefore, this pair will be neglected in further considerations.

Solutions (15) are real when  $K_s^2 + K_c^2 \geq d^2$ , which can be written as

$$-\rho \leq d \leq \rho,\quad (16)$$

where

$$\rho = \sqrt{K_c^2 + K_s^2} = B_1 \sqrt{1 + K^2}; \quad K = K_s/B_1.$$

The solution describing the motion with impacts must fulfill other two conditions, namely

- before impact, the velocity of the mass  $m_1$  must be negative

$$v_1\left(\frac{2\pi n}{\eta}\right) < 0, \tag{17}$$

- during the motion in the time interval between two subsequent impacts, the mass  $m_1$  cannot penetrate the basis

$$x_1(\tau) > -d \text{ for } 0 < \tau < \frac{2\pi n}{\eta}. \tag{18}$$

Conditions (17) and (18) should be checked numerically for the assumed set of parameters describing the system and for many values of the argument  $\tau$  varying with a small step in the range  $0 < \tau < 2\pi n/\eta$ .

#### 4. Stability of periodic motion

As a result of external disturbances, some parameters of motion may alter at the moment of impact: velocities of the masses, displacement of the mass  $m_2$  from its static equilibrium position, and phase shifting of the external forcing. Fig. 3 shows two pairs of trajectories – the undisturbed ( $u_1, u_2$ ) and disturbed ( $d_1, d_2$ ) ones, in the coordinate system with

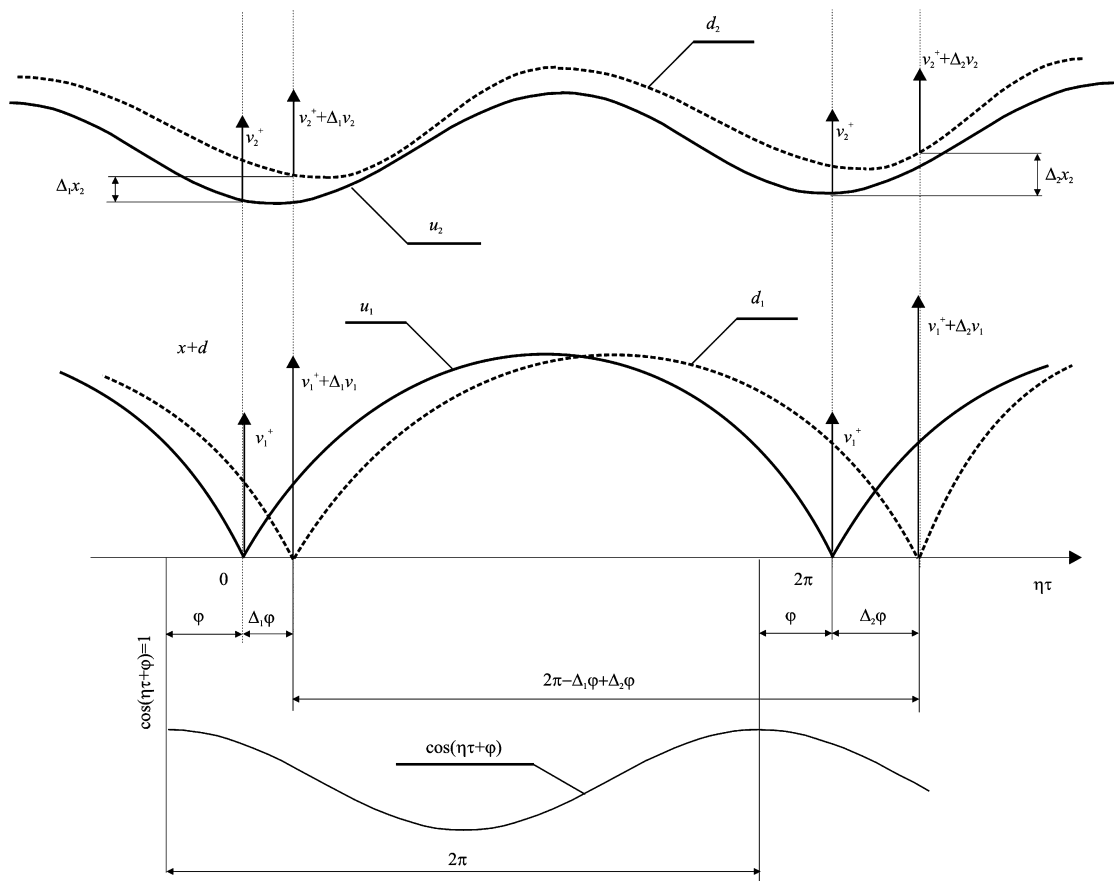


Fig. 3. Undisturbed ( $u_1, u_2$ ) and disturbed ( $d_1, d_2$ ) trajectories of the mass  $m_1$  and  $m_2$ ; example for  $n = 1$ .

$\eta\tau$  on the horizontal axis, and displacements  $x_1 + d, x_2$  on the vertical axis. Below, the function  $\cos(\eta\tau + \varphi)$  of the external forcing is shown additionally.

In the undisturbed case, the mass  $m_1$  hits the basis at  $\eta\tau = 0, 2\pi, \dots$  (example for  $n = 1$ ). When the motion is disturbed, the instant of impact receives an increment, which is denoted by  $\Delta_1\varphi$  at the instant  $\tau = 0$ ; the velocities after impact receive increments denoted by  $\Delta_1v_1$  and  $\Delta_1v_2$ ; the displacement of the mass  $m_2$  at the moment of impact receives an increment denoted by  $\Delta_1x_2$ . On the subsequent impact, the increments were denoted as  $\Delta_2\varphi, \Delta_2v_1, \Delta_2v_2$ , and  $\Delta_2x_2$ . If these increments decrease in time, then the motion of the system is stable.

At the instant  $\tau = 0$ , the displacements of masses and their velocities after impact can be written in the form

$$\begin{aligned} x_1(0) &= -d = A_{11} \cos \psi_1 + A_{12} \cos \psi_2 + B_1 \cos \varphi, \\ x_2(0) &= x_2^+ = A_{21} \cos \psi_1 + A_{22} \cos \psi_2 + B_2 \cos \varphi, \\ v_1(0) &= v_1^+ = -\alpha_1 A_{11} \sin \psi_1 - \alpha_2 A_{12} \sin \psi_2 - \eta B_1 \sin \varphi, \\ v_2(0) &= v_2^+ = -\alpha_1 A_{21} \sin \psi_1 - \alpha_2 A_{22} \sin \psi_2 - \eta B_2 \sin \varphi. \end{aligned} \tag{19}$$

Using these equations, the terms  $A_{11}\cos\Psi_1, A_{12}\cos\Psi_2, A_{21}\cos\Psi_1$  and so on, can be presented as functions of the displacement  $x_2^+$ , velocities  $v_1^+, v_2^+$  and phase shifting  $\varphi$  at the instant  $\tau = 0$ . For  $\tau = 2\pi n/\eta$  (subsequent impact), we have

$$\begin{aligned} x_1\left(\frac{2\pi n}{\eta}\right) &= -d, \\ v_1\left(\frac{2\pi n}{\eta}\right) &= -\frac{1}{k_r} v_1^+, \\ x_2\left(\frac{2\pi n}{\eta}\right) &= x_2^+, \\ v_2\left(\frac{2\pi n}{\eta}\right) &= v_2^+. \end{aligned} \tag{20}$$

In the next step, we have to substitute solutions (5) into (20) and then, to replace terms like  $A_{11}\cos\Psi_1, A_{12}\cos\Psi_2, A_{21}\cos\Psi_1 \dots$  with the functions of  $x_2^+, v_1^+, v_2^+$  and  $\varphi$ . After this, we introduce the increments  $\Delta_1x_2, \Delta_2x_2, \Delta_1v_1, \Delta_2v_1, \Delta_1v_2, \Delta_2v_2, \Delta_1\varphi$  and  $\Delta_2\varphi$ , according to Fig. 3.

Then

- assuming that the equations

$$\begin{aligned} \sin \Delta_1\varphi &= \Delta_1\varphi, \quad \sin \Delta_2\varphi = \Delta_2\varphi, \quad \cos \Delta_1\varphi = 1, \quad \cos \Delta_2\varphi = 1, \\ \sin \frac{\lambda}{\eta}(\Delta_2\varphi - \Delta_1\varphi) &= \frac{\lambda}{\eta}(\Delta_2\varphi - \Delta_1\varphi), \quad \cos \frac{\lambda}{\eta}(\Delta_2\varphi - \Delta_1\varphi) = 1, \end{aligned}$$

are fulfilled as the increments  $\Delta$  are small,

- reducing the terms that do not include the increments and that satisfy Eq. (20) and
- neglecting the terms that include products of the increments as negligibly small,

we obtain a system of four linear equations with the unknowns  $\Delta_1v_1, \Delta_2v_1, \Delta_1v_2, \Delta_2v_2, \Delta_1\varphi, \Delta_2\varphi, \Delta_1x_2$  and  $\Delta_2x_2$

$$[C]\{\Delta_2\} = [D]\{\Delta_1\}, \quad \text{where } \{\Delta_2\} = \begin{Bmatrix} \Delta_2v_1 \\ \Delta_2v_2 \\ \Delta_2x_1 \\ \Delta_2\varphi \end{Bmatrix} \text{ and } \{\Delta_1\} = \begin{Bmatrix} \Delta_1v_1 \\ \Delta_1v_2 \\ \Delta_1x_1 \\ \Delta_1\varphi \end{Bmatrix}. \tag{21}$$

Next, using the substitution

$$\{\Delta_2\} = \beta[I]\{\Delta_1\}, \tag{22}$$

Eq. (21) take the form

$$\{[C^{-1}][D] - \beta[I]\}\{\Delta_1\} = 0. \tag{23}$$

The characteristic equation of matrix (Eq. (23)) is an equation of the fourth degree

$$\beta^4 + r_3\beta^3 + r_2\beta^2 + r_1\beta + r_0 = 0. \tag{24}$$

The use of the following substitution

$$\beta = \frac{w + 1}{w - 1} \tag{25}$$

leads to a new form of the characteristic equation

$$w^4 + s_3w^3 + s_2w^2 + s_1w + s_0 = 0. \tag{26}$$

Then, the condition  $|\beta| < 1$ , which guarantees the diminishing of the increments  $\Delta$ , changes into the condition  $Re(w) < 0$ , which can be easily investigated by means of the Hurwitz stability criterion.

### 5. Model of the cantilever beam with two masses

The numerical calculations, whose results are presented here, deal with a unique case of the 2-DOF system: it consists of a light cantilever beam, on which two concentrated masses are mounted (Fig. 4a). It can be found easily that the stiffness matrix of this beam has the following from

$$\begin{bmatrix} K_{11} & K_{12} \\ K_{21} & K_{22} \end{bmatrix} = \frac{1}{W} \begin{bmatrix} 12EI l_2^3 & -6EI l_2^2(3l_1 - l_2) \\ -6EI l_2^2(3l_1 - l_2) & 12EI l_1^3 \end{bmatrix}, \tag{27}$$

where

$$W = 4l^3 l_2^3 - l_2^4(3l_1 - l_2)^2.$$

The equations of motion take the form

$$\begin{bmatrix} m_1 & 0 \\ 0 & m_2 \end{bmatrix} \begin{Bmatrix} \ddot{x}_1 \\ \ddot{x}_2 \end{Bmatrix} + \begin{bmatrix} K_{11} & K_{12} \\ K_{21} & K_{22} \end{bmatrix} \begin{Bmatrix} x_1 \\ x_2 \end{Bmatrix} = \begin{Bmatrix} F\omega^2 \\ 0 \end{Bmatrix} \cos(\omega t + \varphi). \tag{28}$$

An oscillator that consists of a light cantilever beam of the parameters  $l$  ( $l = l_1$ ),  $EI$ , and a concentrated mass  $m = m_1 + m_2$  mounted at the beam end is the 1-DOF reference system. The coefficient of stiffness of such an oscillator is  $K = 3EI/l^3$ , of course. Referring the masses  $m_1$  and  $m_2$  to the mass  $m$ , and the coefficients  $K_{ij}$  to  $K$ , we obtain dimensionless equations of motion in the form

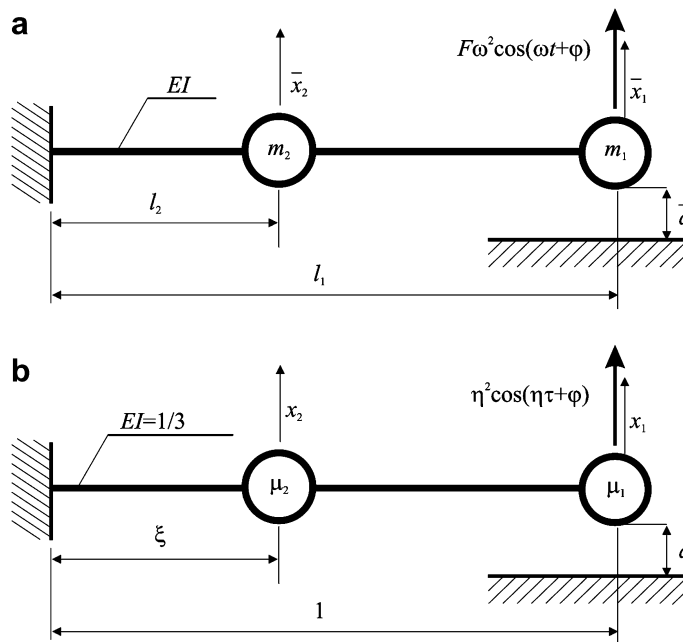


Fig. 4. Cantilever beam with impacts and external excitation: (a) dimensional form; and (b) dimensionless form.

$$\begin{bmatrix} \mu_1 & 0 \\ 0 & \mu_2 \end{bmatrix} \begin{Bmatrix} \ddot{x}_1 \\ \ddot{x}_2 \end{Bmatrix} + \begin{bmatrix} \varsigma_{11} & \varsigma_{12} \\ \varsigma_{21} & \varsigma_{22} \end{bmatrix} \begin{Bmatrix} x_1 \\ x_2 \end{Bmatrix} = \begin{Bmatrix} \eta^2 \\ 0 \end{Bmatrix} \cos(\eta\tau + \varphi). \tag{29}$$

with

$$\begin{aligned} \varsigma_{11} &= \frac{4\xi^3}{4\xi^3 - \xi^6(3 - \xi)^2}, \\ \varsigma_{12} &= -\frac{2\xi^2(3 - \xi)}{12\xi^3 - 3\xi^6(3 - \xi)^2}, \\ \varsigma_{22} &= \frac{4}{4\xi^3 - \xi^6(3 - \xi)^2}, \\ \xi &= l_2/l. \end{aligned}$$

It is important to note that the dimensionless stiffness coefficients of the cantilever beam are functions of one parameter  $\xi$  only. Thus in the stiffness matrix, we have one independent parameter  $\xi$  instead of three ( $\sigma_1, \sigma_2, \sigma_{12}$ ), as it happens in the general case. The relation between  $\sigma_1, \sigma_2, \sigma_{12}$  and  $\xi$  is as follows

$$\begin{aligned} \sigma_1 &= \varsigma_{11} + \varsigma_{12}, \\ \sigma_2 &= \varsigma_{22} + \varsigma_{12}, \\ \sigma_{12} &= -\varsigma_{12}. \end{aligned} \tag{30}$$

### 6. Motion of the 1-DOF system

Fig. 5 refers to a cantilever beam with only one concentrated mass mounted at the end, that is to say, to the system depicted in Fig. 4b, with the following parameters:  $\mu_1 = 1, \mu_2 = 0$ . In Fig. 5a it has been shown how the character of the system motion depends on values of the parameters  $\eta$  and  $d$ . If the point  $(\eta, d)$  lies within one of the regions denoted by numbers  $n = 1, 2, 3, \dots$ , then the motion of the system will be periodic, with a period  $1, 2, 3 \dots$  times longer than the period of the excitation force. If the point  $(\eta, d)$  lies beyond the regions of periodic motion, then the system will be characterized by chaotic, quasi-chaotic or periodic motion that does not fulfill the assumption of identity of all impacts (cf. the description of the Peterka’s method). The line denoted by  $B_1$  shows amplitude of forced vibrations (see Eq. (8)). If a value of the parameter  $d$  is higher than  $B_1$ , then besides periodic motion with impacts, periodic motion without impacts is also possible, which means that we have a coexistence of attractors, and the kind of motion (with impacts or without) depends of course on the initial conditions. In Fig. 5b an example of periodic motion with impacts for the system whose parameters are  $d = 0$  and  $\eta = 4$  (denoted by point  $A$  in Fig. 5a) is shown. The time unit on the horizontal axis is the

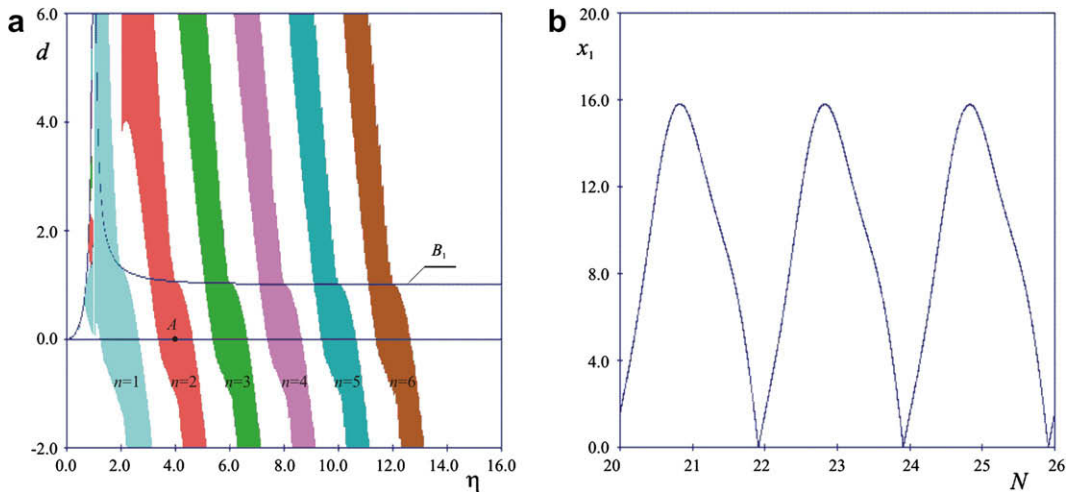


Fig. 5. Periodic solutions for the 1-DOF system: (a) regions of existence; and (b) example of time series,  $d = 0, \eta = 4.0$ .

period of excitation force  $T = 2\pi/\eta$ ; number  $N$  stands for the number of such periods. As can be seen, according to Fig. 5a, it is periodic motion with period 2 ( $n = 2$ ). As each impact initiates free vibrations, the total displacement of the system is a sum of forced vibrations with the frequency  $\eta$  and free vibrations with the frequency  $\alpha_1$ . It is worth noticing that the regions of periodic motion for the values of  $d$  close to zero are located in the neighborhood of the frequencies  $\eta$  equal to even multiples of the eigenvalue  $\alpha_1 = 1$ .

### 7. Motion of the 2-DOF system

Fig. 6a presents regions of periodic motion for the 2-DOF cantilever beam (Fig. 4b) with the parameters  $\zeta = 0.5, \mu_1 = 0.9, \mu_2 = 0.1$ . As the mass  $\mu_2$  is low compared to  $\mu_1$ , it can be noticed that the regions of periodic motion of the 2-DOF system have a shape of the respective regions for the 1-DOF system, from which certain fragments have been deleted (cf. Fig. 5a). The reason why the regions of periodic motion for the 2-DOF system are smaller is of course the fact that each impact generates free vibrations which are a superposition of vibrations with the frequencies  $\alpha_1$  and  $\alpha_2$ . The total displacement of the system (in the time intervals between impacts) is thus a superposition of not two but three harmonic motions and the range of parameters  $d$  and  $\eta$ , for which their mutual synchronization is possible, is lower than for the 1-DOF system. In Fig. 6b an example of periodic motion with impacts for the system of parameters  $d = 0$  and  $\eta = 4.2 = 4.0 \times \alpha_1$  (denoted by point A in Fig. 6a) is shown. Apart from the displacement  $x_1$ , the displacement  $x_2$  of the additional mass is presented as well. As can be seen, the time history of the displacement  $x_1$  of the mass that impacts against the basis is similar to the time history of the displacement in Fig. 5b – only a difference in amplitudes is visible. In the displacement  $x_2$  shown in Fig. 6b, one can see how large the part of free vibrations with the frequency  $\alpha_2$  is.

Fig. 7 depicts the regions in which periodic motion with impacts exists for the 2-DOF system defined by the parameters  $\mu_1 = 0.5, \mu_2 = 0.5$  (both masses are identical) and  $\zeta = 0.348$  (Fig. 7a) or  $\zeta = 0.305$  (Fig. 7b). In Fig. 7a wide regions of periodic motion can be observed, especially for low values of  $d < 2$  (for the value of parameter  $\zeta = 0.348$ , the ratio of eigenfrequencies of the system is  $\alpha_2/\alpha_1 = 8.0$ ). Contrary, in Fig. 7b drawn for the system with  $\zeta = 0.305$  ( $\alpha_2/\alpha_1 = 9$ ), the regions of periodic motion are substantially smaller. It seems clear that the relations between the values  $\alpha_2, \alpha_1$  and  $\eta$  exert a strong influence on the periodicity of the 2-DOF system motion.

### 8. Eigenfrequencies

In the light of the fact that dimensionless coefficients of stiffness of the beam are functions of one parameter only, whereas both dimensionless masses are related by the relationship  $\mu_1 + \mu_2 = 1$ , the eigenfrequencies  $\alpha_1$  and  $\alpha_2$  of the

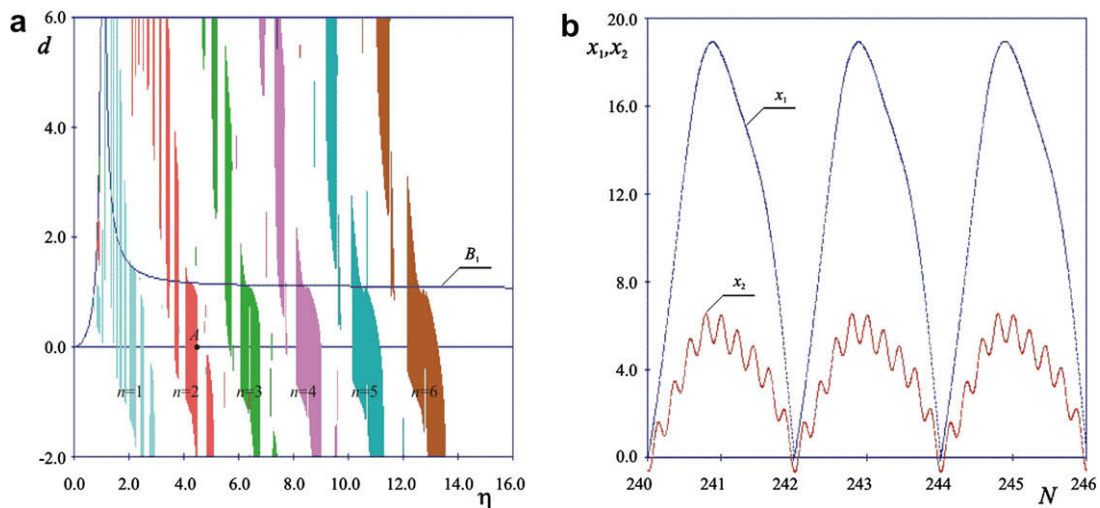


Fig. 6. Periodic solutions for the 2-DOF system: (a) regions of existence,  $\mu_1 = 0.9, \mu_2 = 0.1, \zeta = 0.5$ ; and (b) example of time series,  $d = 0, \eta = 4.2$ .

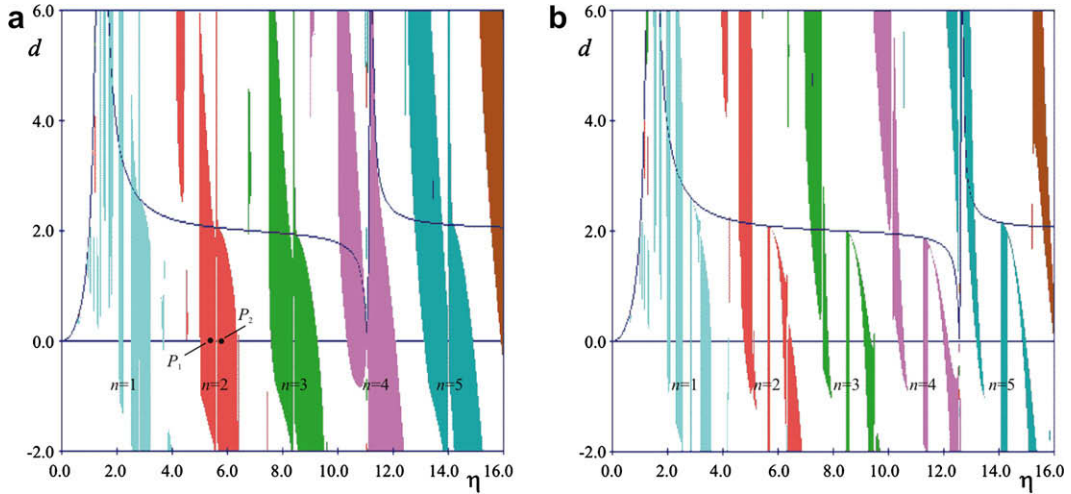


Fig. 7. Regions of the periodic solution for the 2-DOF system,  $\mu_1 = \mu_2 = 0.5$ : (a)  $\zeta = 0.348$ ; and (b)  $\zeta = 0.305$ .

system in Fig. 4 can be presented as functions of two parameters:  $\zeta$  and  $\mu = \mu_1/(\mu_1 + \mu_2)$ . Fig. 8a shows a dependence between values of the parameters ( $\mu, \zeta$ ) and a value of the ratio of eigenfrequencies  $\lambda = \alpha_2/\alpha_1$ . Points with the coordinates ( $\mu, \zeta$ ) lying on the borders between light and dark regions correspond to the systems for which the ratio of eigenfrequencies  $\lambda = \alpha_2/\alpha_1$  is a natural number. For instance, for point  $U (\mu = 0.5, \zeta = 0.605)$ , the value of  $\lambda = 7.0$ . The last border between the light and dark region was calculated for  $\lambda = 19$ . For higher values of  $\lambda$ , calculations were not conducted.

**9. Relation of the frequency ratio – periodicity**

In Fig. 8b, regions of periodic motion with impacts for the system defined by the parameters  $\mu = 0.5$  (both masses are identical) and  $d = 0.0$  are depicted. The frequency of excitation force  $\eta$  (horizontal axis) and the parameter  $\zeta$  that defines the position of the additional mass are on the coordinate axes.

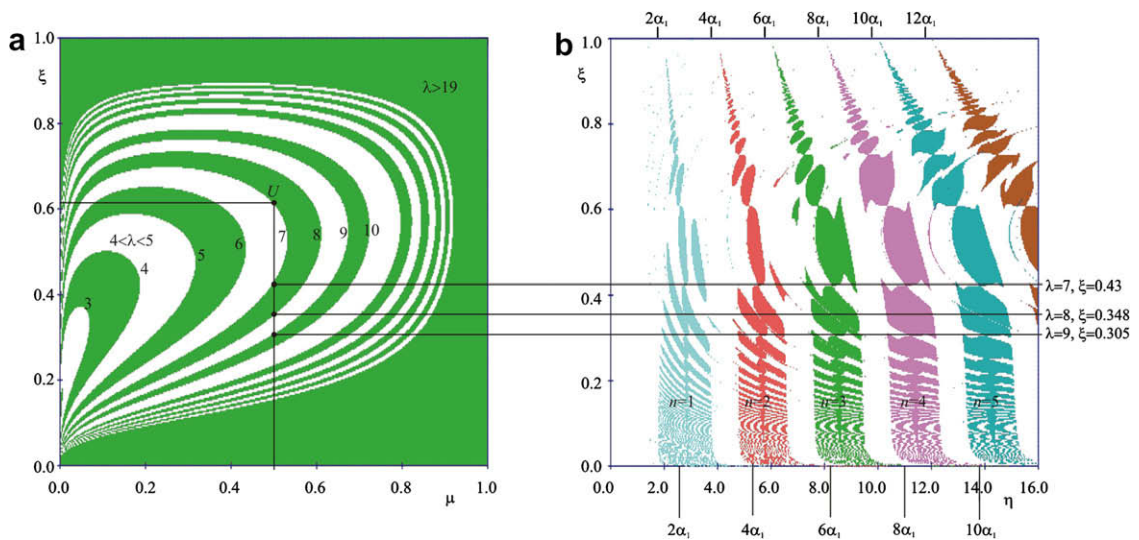


Fig. 8. Relation between eigenfrequencies and periodicity of motion: (a) frequency ratio  $\lambda$ ; and (b) regions of stable solutions for  $d = 0$ ,  $\mu = 0.5$ .

The dependence of the position of periodic motion regions on the relation between the frequency value  $\eta$  and the value of the fundamental eigenvalue  $\alpha_1$  can be seen clearly. For low values of the parameter  $\xi$ , the additional mass is close to the fixed end of the beam and its vibrations hardly affect the motion of the second mass. The behavior of the system resembles the behavior of the 1-DOF system with the mass  $\mu_1 = 0.5$ . The eigenfrequency of this system is  $\alpha_1 = 1.41$  and (as can be seen) regions of periodic motion for low values of the parameter  $\xi$  are in the vicinities of values of  $\eta$  equal to its multiples: 2.82, 5.64, 8.46, etc. For high (close to 1) values of the parameter  $\xi$ , the additional mass is close to the free end of the beam and its vibrations are nearly the same as the vibrations of the mass fixed to this beam end. The system behaves almost as the 1-DOF system with the mass  $\mu_1 = 1.0$  and  $\mu_2 = 0.0$ . The eigenfrequency of this system is  $\alpha_1 = 1.0$  and (as can be seen) regions of periodic motion for high values of the parameter  $\xi$  are in the vicinities of values of  $\eta$  equal to its multiples: 2, 4, 6, etc.

The dependence of the position of regions of periodic motion and the frequency value  $\eta$ , as well as the ratios of eigenvalues  $\lambda$  are visible as well: when the value of  $\lambda$  is close to an odd number, then gaps occur in regions of periodic motion; for systems in which  $\lambda$  is close to an even natural number, wide ranges of the values of  $\eta$  in which the system motion is periodic can be seen. The position of ranges of periodic motion for  $\lambda = 8$  and 9 can be compared to Fig. 7 for  $d = 0.0$ .

### 10. Origins of periodicity

Fig. 9a shows regions of the parameters  $\eta$  and  $\xi$  for which there exists a periodic solution ( $n = 2$ ) that fulfils the condition that the mass  $m_1$  cannot penetrate the basis (Eq. (18)). The solution can be stable or not. Fig. 9b is an enlarged fragment of Fig. 8b and it presents regions of the parameters  $\eta$  and  $\xi$  for which a periodic solution satisfies the stability condition additionally. One can easily observe that only for a small region of the parameters  $\eta$  and  $\xi$ , the cause why a periodic solution does not exist is the condition that the basis is not penetrated. It occurs, for instance, for points  $D_1$  and  $D_2$  ( $\xi = 0.69, \eta = 4.95$  and  $\eta = 0.51$ , correspondingly). In principle, the solution stability decides about differences in the extent of the regions denoted in Fig. 9a and b. That is to say, for point  $R$  ( $\eta = 6.0, \xi = 0.348, \lambda = 8$ ), a periodic solution with period 2 exists, does not penetrate the basis and is stable – the system this point corresponds to operates within a wide region of periodic motion. The system to which point  $S$  ( $\eta = 5.63, \xi = 0.305, \lambda = 9$ ) corresponds is characterized by periodic motion with period 2, however even a slight (often unintended) alternation in the frequency of excitation force introduces the system into the white field where the periodic motion is unstable; the system motion is quasi-periodic or chaotic here. Exemplary Poincare maps are depicted in Fig. 10. The map shown in Fig. 10a is drawn for the system with quasi-periodic motion, to which point  $Q_1$  in Fig. 9b ( $\eta = 5.9, \xi = 0.305$ ), situated close to point  $S$ , corresponds. A further increase in the frequency of excitation force introduces the system into the chaotic motion region: in Fig. 10b (point  $Q_2, \eta = 5.95, \xi = 0.305$ ), a chaotic attractor can be seen (20000 points have been presented).

While analyzing the results obtained with the Peterka's method, the authors' attention was drawn to narrow regions of non-periodic motion going across the centers of periodic motion regions, which can be seen in Fig. 7a (e.g., for  $\eta = 5.6$  in case of  $n = 2$ ). In Fig. 9 this region separates points  $P_1$  and  $P_2$  and, as can be seen, the cause of its existence

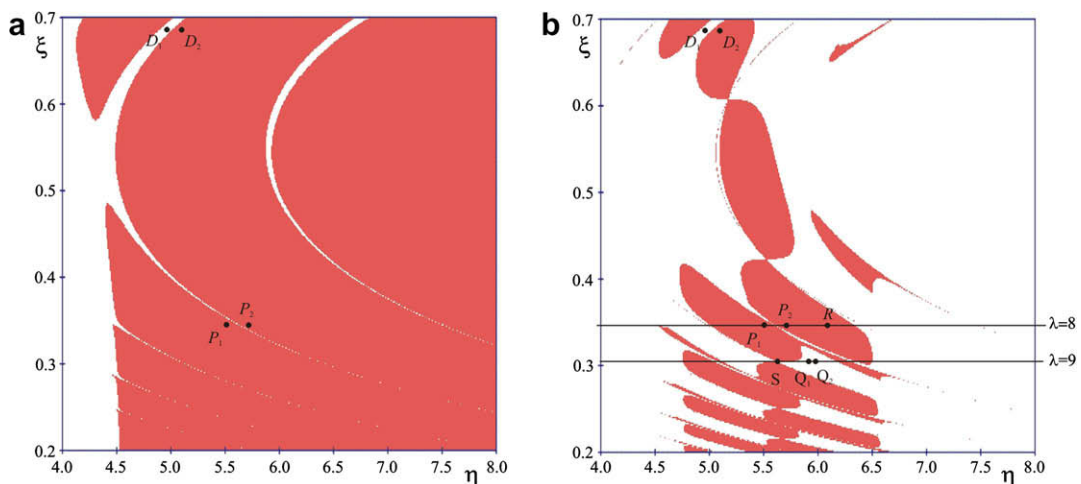


Fig. 9. Regions in which: (a) the solution does not penetrate the basis; and (b) the solution is stable,  $d = 0, \mu = 0.5, n = 2$ .

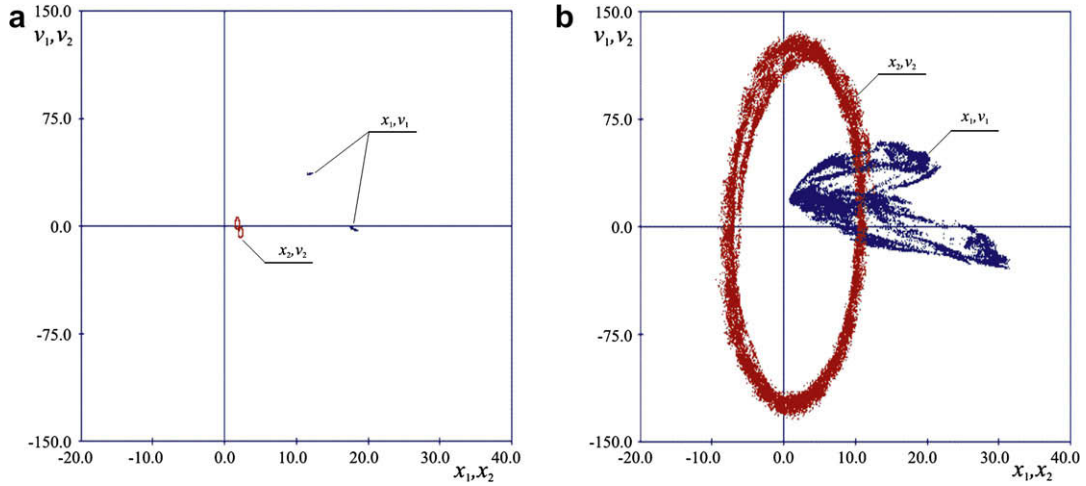


Fig. 10. Poincaré maps for  $d = 0$ ,  $\mu = 0.5$ ,  $\zeta = 0.305$ : (a)  $\eta = 5.9$ ; and (b)  $\eta = 5.95$ .

lies in the fact that the condition of non-penetration of the basis is not satisfied. In Fig. 11 time histories of the solutions that correspond to these points:  $P_1$  ( $\eta = 5.5, \zeta = 0.3485$ ) and  $P_2$  ( $\eta = 5.7, \zeta = 0.3485$ ) are drawn. As one can notice, the time histories of the displacement of the mass  $\mu_1$  are very similar in both figures, whereas the time histories of the displacement of the mass  $\mu_2$  differ much: at the impact instant, this mass moves either in phase with  $\mu_1$ , or in antiphase.

### 11. Comparison of the methods

During the calculations, whose results are presented in this paper, two qualitatively different methods for motion analysis of the vibrating 2-DOF system were applied. To compare the results obtained with these two methods, Fig. 12 has been drawn. Fig. 12a presents a part of Fig. 8a, in the range  $-2 < d < 2$ . In Fig. 12b a bifurcation diagram for the system Fig. 12a corresponds to has been shown, assuming that  $d = 0.0$ . The vertical lines that for  $d = 0.0$  denote these values of the frequency  $\eta$  (determined with the Peterka’s method) for which the periodic motion transforms into the non-periodic one and vice versa, go also across the borders of ranges of the periodic and non-periodic motion on the bifurcation diagram obtained by means of integration of motion equations with the Runge–Kutta method. This diagram is shown as a confirmation of correctness and suitability of both the methods applied.

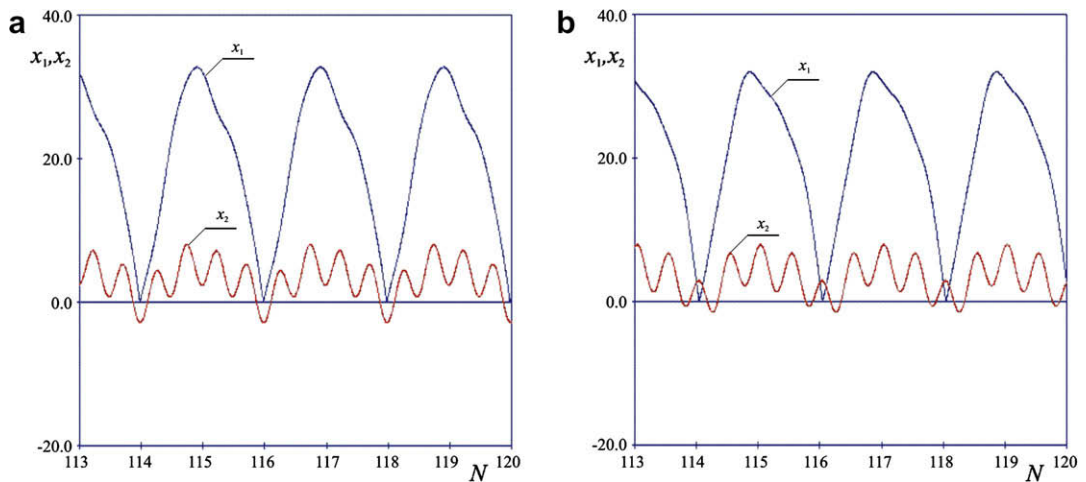


Fig. 11. Time series for  $d = 0$ ,  $\mu = 0.5$ ,  $\zeta = 0.3485$ : (a)  $\eta = 5.5$ ; and (b)  $\eta = 5.7$ .

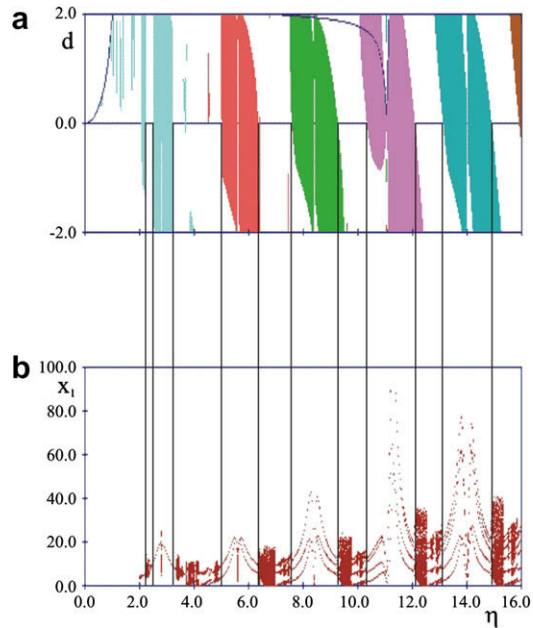


Fig. 12. Comparison of the methods: (a) regions of the stable solution,  $\mu = 0.5$ ,  $\xi = 0.348$ ; and (b) the bifurcation diagram,  $\mu = 0.5$ ,  $\xi = 0.348$ ,  $d = 0$ .

## 12. Conclusions

The results of the conducted calculations allow for drawing the following conclusions:

1. Stable solutions that describe motion with impacts of the mechanical 2-DOF system exist in considerably wide ranges of parameters describing this system.
2. The position and size of regions of periodic motion depend strongly on relations between the frequency of excitation force  $\eta$  and the eigenvalues  $\alpha_1$  and  $\alpha_2$ . To obtain stable and periodic motion with impacts, the system should be designed in such a way that the frequency of excitation force  $\eta$  is an even multiple of the fundamental eigenvalue  $\alpha_1$ , and the higher eigenvalue  $\alpha_2$  is an even multiple of the excitation force frequency  $\eta$ .
3. The system exhibits adaptability, owing to which stable periodic solutions exist even if the above-mentioned conditions are not strictly fulfilled, i.e., when  $\eta \approx 2n \times \alpha_1$  and  $\alpha_2 \approx 2m\eta$ .
4. The basic cause why the system motion is chaotic or quasi-chaotic is the instability of the existing periodic solution to equations of motion.
5. The conducted calculations show a good agreement of the results obtained with two qualitatively different methods for analysis of the system under investigation: the Peterka's method and the numerical integration of equations of motion.

## Acknowledgement

This study has been supported by the Polish Department for Scientific Research (DBN) under Project No. N501 037 31/2508.

## References

- [1] Aidanpaa JO, Gupta RB. Periodic and chaotic behaviour of a threshold-limited two-degree-of-freedom system. *J Sound Vib* 1993;165:305–7.
- [2] Arnold RN. The acceleration absorber. In: *Proceedings of the ninth international conference of applied mechanics*; 1956. p. 367–72.

- [3] Bapat CN. Periodic motions of an impact oscillator. *J Sound Vib* 1998;209:43–60.
- [4] Blazejczyk-Okolewska B, Czolczynski K, Kapitaniak T. Classification principles of types of mechanical systems with impacts – fundamental assumptions and rules. *Euro J Mech A/Solid* 2004;23:517–37.
- [5] Blazejczyk-Okolewska B, Czolczynski K, Kapitaniak T, Wojewoda J. Chaotic mechanics in systems with impacts and friction. World scientific series in non-linear science, series A. Singapore: World Scientific Publishing Co; 1999.
- [6] Blazejczyk-Okolewska B, Kapitaniak T. Co-existing attractors of impact oscillator. *Chaos, Solitons & Fractals* 1998;9:1439–43.
- [7] Brach R. Mechanical impact dynamics: rigid body collisions. New York: John Wiley and Sons; 1991.
- [8] Cempel C. The multi-unit impact damper: equivalent continuous force approach. *J Sound Vib* 1974;34:199–209.
- [9] Chin W, Ott E, Nusse HE, Grebogi C. Grazing bifurcations in impact oscillators. *Phys Rev E* 1994;50:4427–44.
- [10] Czolczynski K, Kapitaniak T. Influence of the mass and stiffness ratio on a periodic motion of two impacting oscillators. *Chaos Solitons & Fractals* 2003;17:1–10.
- [11] Czolczynski K, Kapitaniak T. On the existence of a stable periodic solution of two impacting oscillators with damping. *Int J Bifurcat Chaos* 2004;14:3931–47.
- [12] Czolczynski K, Kapitaniak T. On the influence of the resonant frequencies ratio on stable periodic solutions of two impacting oscillators. *Int J Bifurcat Chaos* 2006;16:3707–15.
- [13] Dabrowski A. The energy space, energy flow and synchronization. *Mech Mechan Eng* 2005;9:187–205.
- [14] de Souza SLT, Caldas IL, Viana RL, Balthazar JM, Brasil RMLRF. Basins of attraction changes by amplitude constraining of oscillators with limited power supply. *Chaos, Solitons & Fractals* 2005;26:1211–20.
- [15] de Weger J, van de Water W, Molenaar J. Grazing impact oscillations. *Phys Rev E* 2000;62:2030–41.
- [16] di Bernardo M, Feigin MI, Hogan SJ, Homer ME. Local analysis of C-bifurcations in  $n$ -dimensional piecewise-smooth dynamical systems. *Chaos, Solitons & Fractals* 1999;10:1881–908.
- [17] Fang W, Wickert JA. Response of a periodically driven impact oscillator. *J Sound Vib* 1994;170:397–409.
- [18] Feigin MI. Doubling of the oscillation period with C-bifurcations in piecewise continuous systems. *PMM* 1970;34:861–9.
- [19] Foale S, Bishop SR. Dynamical complexities of forced impacting systems. *Phil Trans Royal Soc Lond A* 1992;338:547–56.
- [20] Goldsmith W. Impact. London: Arnold LTD; 1960.
- [21] Hinrichs N, Oestreich M, Popp K. Dynamics of oscillators with impact and friction. *Chaos, Solitons & Fractals* 1997;8:535–58.
- [22] Ivanov AP. Impact oscillations: linear theory of stability and bifurcations. *J Sound Vib* 1994;178:361–78.
- [23] Isomaki H, Boehm J, Raty R. Devil's attractors and chaos of a driven impact oscillator. *Phys Lett A* 1985;107:343–6.
- [24] Jerrelind J, Stensson A. Non-linear dynamics of parts in engineering systems. *Chaos, Solitons & Fractals* 2000;11:2413–28.
- [25] Koizumi K. Analysis of vibration with collision and applications to leaf beating machine. Doctor thesis, University of Tokyo, Precision Mechanical Engineering; 1980 [in Japanese].
- [26] Masri SF. Analytical and experimental studies of multi-unit impact dampers. *J Acoust Soc Am* 1964;45:1111–7.
- [27] Masri SF, Caughey TK. On the stability of the impact damper. *J Appl Mech* 1966;33:586–92.
- [28] Moon FC, Shaw SW. Chaotic vibrations of a beam with non-linear boundary condition. *Int J Non-linear Mech* 1983;18:465–77.
- [29] Nordmark AB. Non-periodic motion caused by grazing incidence in an impact oscillator. *J Sound Vib* 1991;145:279–97.
- [30] Park WH. Mass-spring-damper response to repetitive impacts. *Trans ASME J Eng Indust* 1967:587–96.
- [31] Peterka F. An investigation of the motion of impact dampers, paper I, II, III. *Strojnicku Casopis XXI* 1971:c.5.
- [32] Peterka F, Blazejczyk-Okolewska B. Some aspects of the dynamical behavior of the impact damper. *J Vib Contr* 2003;11:459–79.
- [33] Peterka F, Vacik J. Transition to chaotic motion in mechanical systems with impacts. *J Sound Vib* 1992;154:95–115.
- [34] Popplewell N, Liao M. A simple design procedure for optimum impact dampers. *J Sound Vib* 1991;147:519–26.
- [35] Shaw SW. Forced vibrations of a beam with one-sided amplitude constraint: theory and experiment. *J Sound Vib* 1985;99:199–212.
- [36] Shaw SW, Holmes PJ. A periodically forced piecewise linear oscillator. *J Sound Vib* 1983;90:129–55.
- [37] Thompson JMT, Ghaffari R. Chaos after period-doubling bifurcations in the resonance of an impact oscillator. *Phys Lett A* 1982;91:296–9.
- [38] van de Vorst ELB, van Campen DH, de Kraker A, Fey RHB. Periodic solutions of a multi-DOF beam system with impact. *J Sound Vib* 1996;192:913–25.